Contents list available at CBIORE journal website

International Journal of Renewable Energy Development

Journal homepage: https://ijred.cbiore.id

Research Article

Effect of solution pH and concentration of Dewandaru fruit extract as a natural dye on optical characteristics and performance of dye-sensitized solar cells

Dadi Rusdiana[a], Eka Cahya Prima[b]*, Muhammad N Ikhsan[a], Andhy Setiawan[a], Endi Suhendi[a], Arip Nurahman[b,c], Semuel Unwakoly[d], Arramel Arramel[e]

[a]*Department of Physics, Universitas Pendidikan Indonesia, Bandung, Indonesia*

[b]*Department of Science Education, Universitas Pendidikan Indonesia, Bandung, Indonesia*

[c]*Department of Physics Education, Institut Pendidikan Indonesia, Garut, Indonesia*

[d]*Chemistry Education Study Program, Universitas Pattimura, Ambon, Indonesia*

[e]*Center of Excellence Applied Physics and Chemistry, Nano Center Indonesia, Indonesia*

Abstract. Given growing global energy demand and the need for sustainable solutions, solar energy is a promising alternative. Dye-sensitized solar cells (DSSC) are a cost-effective photovoltaic technology, and natural dyes as sensitizers have significant potential to improve their efficiency. This study explores the use of a natural dye from the Dewandaru fruit (*Eugenia uniflora*) in DSSCs by varying pH and concentration. Natural dyes offer an environmentally friendly, sustainable alternative to synthetic dyes, which are often expensive and less eco-friendly. In this research, Dewandaru fruit extract was used to sensitize TiO_2 photoanodes, and the effects of varying pH (1.00, 1.66, 2.27, and 3.00) and dye concentrations (2.5, 5.0, 7.5, and 10%) on optical properties and performance were analyzed. UV-Vis spectroscopy, FTIR, cyclic voltammetry, and J-V measurements were used to assess absorbance, energy levels, and efficiency. Optical characterization results showed that changes in pH and concentration can affect the dye's absorbance and energy band gap. The dye achieved optimal DSSC performance at pH 3.00, yielding a Voc of 0.425 V, Jsc of 0.053 mA/cm², a fill factor of 68.7%, and an efficiency of 0.01548%. The best dye concentration was 10%, achieving a Voc of 0.45 V, a Jsc of 0.105 mA/cm², a fill factor of 69.0%, and an efficiency of 0.0322%. The statistical analysis indicates that pH has a substantial positive effect on DSSC efficiency and band gap energy. Moreover, dye concentration significantly affects DSSC efficiency, light-harvesting efficiency, Jsc, and fill factor, with the most substantial effects on efficiency and Jsc. However, concentration appears to have a smaller effect on dye absorbance, band gap energy, and HOMO/LUMO values. The study indicates that Dewandaru fruit extract has potential as a natural dye for DSSCs, with performance varying with pH and concentration.

Keywords: Concentration, Dye-sensitized solar cells, *Eugenia uniflora,* Natural dye, pH solvent

Received: 16th August 2025; Revised: 6th January 2026; Accepted: 17th July 2026; Available online: 7th Sept 2026

1. Introduction

Over the past few years, the world's population has grown rapidly, driving up energy demand. As a result, Earth's fossil fuel reserves are being depleted quickly. Energy consumption is estimated to grow from 19.2 TW per year to 24.6 TW per year from 2015 to 2040 (Carella *et al*., 2018; Sukarno *et al*., 2015). In addition to depleting supplies due to massive use, fossil fuels are a source of electrical energy that produces greenhouse gas emissions such as carbon dioxide, carbon monoxide, and sulfur dioxide, which result in global warming (Omer, 2012; Singh *et al*., 2013).

Technological sources that are abundant and do not cause adverse environmental effects are needed to achieve a sustainable life (Kabeyi & Olanrewaju, 2022). Solar energy can be a promising solution because it is a clean, inexhaustible energy source with no associated costs (O'Regan & Grätzel, 1991). Solar energy can be converted directly into heat, so researchers use it as a power source (Rahman. *et al.* 2020). Dye-sensitized Solar Cells (DSSC) are among the most cost-effective technologies studied in recent years (Yan *et al.*, 2025). Manufacturing these solar cells is relatively low-cost because they use low-cost materials, and assembly is easy (Rajkumar et al., 2025).

Third-generation cells aim to surpass the efficiency limits of previous generations while being cost-effective (Sharma et al., 2022). The DSSC, first developed in 1991 by O'Regan and Grätzel, had an energy conversion efficiency of 7% (O'Regan & Grätzel, 1991). Nanostructured metal oxide films, which form the basis of DSSC devices, are sensitized by adsorbed dyes to harvest visible light. DSSC components include transparent conductive glass as a substrate, a wide-band-gap

* Corresponding author
Email: ekacahyaprima@upi.edu (E. C.Prima)

semiconductor, an electrolyte, and a counter electrode (Prima *et al*., 2024). Common transparent conductive glass substrates include fluorine-doped tin oxide ($F:SnO_2$) and Indium Tin Oxide ($In:SnO_2$) (Bekele & Sintayehu, 2022). Among semiconductor materials, TiO_2 is widely used in these devices. The TCO (Transparent Conducting Oxide) coating on the substrate serves as both the electrode and the counter electrode. The counter electrode is coated with an electrolyte commonly used as I^-/I_3^- (iodide/triiodide) to accelerate the redox reaction (Prima *et al*., 2020). The dye is oxidized upon absorbing photons, and the resulting excited electrons are injected into the semiconductor conduction band. After injection, the electrolyte collects electrons through redox reactions, completing the cycle of converting light into electricity (Bhogaita *et al., 2*016).

The pigment in dye-sensitized solar cells (DSSCs) plays a crucial role in determining their efficiency. The efficiency of DSSCs is significantly influenced by the ability of the sensitizer to absorb a wide range of the solar spectrum (Alessa *et al*., 2024). Generally, Ruthenium-bipyridyl is used as a dye in DSSC devices, producing high energy conversion efficiencies of around 11-12% (Saud *et al*., 2024; Shruti Singh *et al*., 2021). Ruthenium (Ru) is a suitable sensitizer for DSSCs due to its strong charge-transfer absorption and high efficiency in the visible. Because ruthenium (Ru) is expensive, researchers have begun developing metal-free organic sensitizers. Natural dyes are a good alternative to Ruthenium (Ru) as sensitizers. Natural dyes can be found in fruits, flowers, leaves, roots, and other plant parts (Calogero *et al*., 2015). The choice of natural dyes as sensitizers is not only due to their low cost but also to their ease of manufacture, making them a practical solution. Pigments such as anthocyanins and carotenoids in natural dyes make the pigments photoactive and can be adsorbed on the surface of TiO_2 (Eka *et al*., 2013). Although these natural dyes are suitable for DSSCs, their chemical structures pose a significant problem because they are difficult to modify in vitro. This is because plants evolve naturally (Prima *et al*., 2018).

Because of these limitations, alternatives are needed to maximize the function of natural dyes in DSSCs, such as changes in pH and concentration (Kumara *et al*., 2017). The type of solvent is essential in DSSC fabrication because the acidity level can affect the absorption spectrum of the dye as well as the bonding of the dye with TiO_2, which will have an impact on the optical characteristics and performance of the DSSC (Bekele & Sintayehu, 2022; Teja *et al*., 2023). The same thing will also happen if there is a change in the concentration of the extractor in the solvent (Faqih *et al.,* 2019; Muryani *et al.,* 2019).

Dewandaru fruit (Eugenia uniflora), also known as pitanga, is rare in Indonesia (Seidemann, 2005). This fruit, belonging to the Myrtaceae family, is native to Central and South America, particularly Brazil, Argentina, and Paraguay. (da Silva Diniz *et al*., 2014). Although it is appreciated for its health benefits and ornamental potential, it is not widely known or cultivated in Indonesia. As a sensitizer, this is one of the first systematic investigations of its optical and photovoltaic characteristics. (Magalhães et al., 2025). While several other natural dyes, such as anthocyanins from blackberries, mangosteen, and hibiscus, have been previously explored (Maiaugree *et al*., 2015; Rajkumar *et al*., 2025; Raturi & Fepuleai, 2010). Dewandaru remains underreported despite its high anthocyanin and phenolic content (Santoso et al., 2020)

This fruit is also called Brazilian cherry because it mainly grows in Brazil. Pitanga fruit contains phenolic compounds, including 69 mg of anthocyanins per 100 g. The content is higher than that of frozen grapes (*Vitis vinifera*), which is 30.9 mg/100 g, and strawberries (Fragaria vesca), which is 22.8 mg/100 g (Bagetti *et al.,* 2011). Anthocyanin reactivity depends on their structure and several factors, including pH, temperature, light, oxygen, and enzymes. pH is an essential factor affecting anthocyanin stability. Generally, anthocyanins are more stable in acidic environments (pH < 7). The advantage of anthocyanin as a natural colorant in DSSC fabrication lies in its structure's carbonyl and hydroxyl groups, which facilitate attachment to the TiO_2 layer, increasing energy conversion efficiency (Pramananda *et al*., 2021).

This research investigated the potential of a natural dye derived from Dewandaru fruit for DSSCs by analyzing how pH levels and dye concentrations affect optical properties and device performance, aiming to provide a sustainable alternative to synthetic dyes. We report the first-ever use of Dewandaru (*Eugenia uniflora*) fruit extract as a dye in DSSC applications. Additionally, our research simultaneously investigates two influential parameters: pH and concentration, which have not been commonly investigated in previous literature. We provide greater insight into dye optimization by analyzing how these parameters affect optical properties, HOMO-LUMO energy levels, and photovoltaic performance. We also compare performance with a commercial dye (N719) under the same conditions. We believe this comprehensive approach represents a meaningful advance in exploring low-cost, eco-friendly photosensitizers for DSSCs and provides new directions for using underutilized tropical fruits in green energy technologies.

2. Materials and methods

2.1 Dye Extraction

We washed and cleaned 1 kilogram of dewandaru fruit samples, then removed the seeds. After seed removal, 750 grams of dewandaru fruit was dried in a vacuum oven for 3 days and crushed to a smooth consistency in a blender (Cosmos, 450W). After pulverizing the dried dewandaru fruit, 245 grams of powder were obtained. To prepare pH variations, methanol was mixed with acetic acid at a 95:5 (%v/v) ratio to a total volume of 200 mL, divided into four equal parts; HCl (Merck) was then added as an acid control (López et al., 2017). The four solutions had a pH of 1.00, 1.66, 2.27, and 3.00. We added the fine powder to each solvent at a 1:20 (w/v) ratio, stirred with a magnetic stirrer at 500 rpm until evenly mixed, then left to stand at room temperature for 7 days. Afterward, the solution was filtered through Whatman filter paper (Merck, 11 μm pore size) using the Filtration Buncher Vacuum Kit at 0.1 bar. The thick extract obtained from the filtration was centrifuged at 4000 rpm for 10 minutes. The results were then characterized, and one dye solution was prepared at concentrations of 2.5, 7.5, and 10 (% w/v) using the same manufacturing process. For the control pigment, an N719 dye-photosensitizer was prepared in a solution containing 19 mL H2O, 80 mL MeOH, and 1 mL HCl, resulting in a 2.2 mM pigment concentration (Prima et al., 2024)

2.2 Film Preparation

A TiO_2 nanoparticle electrode on FTO (Pilkington, TEC-8, 8 Ω/sq, received from Yingkou OPV Tech New Energy Co., Ltd., China) was immersed in 10 mL of dye solution. The FTO substrate, in this case, Pilkington TEC-8 glass, serves as a transparent conductive oxide, allowing light to pass through while providing an electrical contact to collect the generated electrons. Its low sheet resistance (8 Ω/sq) minimizes resistive losses, thereby improving overall cell performance. Similar works on using TiO_2-adsorbed FTO substrate were reported by Chen *et al.* (2020); Chen *et al.* (2023), and Zhang *et al.* (2020).

The maceration was carried out in a refrigerator for 7 days to prevent the dye from evaporating. After immersion, the photoanode was cleaned with 2-propanol using a cotton bud without scratching the thin film, then dried. ITO conductive transparent glass (6Ω/sq, 90% transmittance) was cut into a 1×2 cm size for counter electrode preparation. The cut glass was then cleaned in an ultrasonic cleaner for 15 minutes. After cleaning, the glass substrate was rinsed with 2-propanol, then dried.

The counter electrode was prepared by dripping 25 μl of a 20 mM hexachloroplatinic acid (Aldrich) solution onto the cut ITO substrate. The solution was evenly applied to the conductive part of the glass substrate. Then, the substrate was spin-coated at 4000 rpm for 30 seconds, followed by heating at 80°C for 5 minutes. When the temperature had returned to normal, the platinum electrode was annealed at 380°C for 30 minutes. The annealed counter electrode was allowed to dry.

2.3 Fabrications

Around the TiO_2 thin film, Low Temperature Thermoplastic Sealant (25μm thickness, Dyesol) was applied, and then EL-HPE electrolyte (Dyesol, mixture of solvents, a redox couple (triiodide/iodide), and additives including acetonitrile and valeronitrile as solvents. The redox couple is I_3^-/I^-, and the additives included inorganic and organic iodide salts and pyridine derivatives, which were added in about 20 μl. The two electrodes were then joined and clamped with a paper clip. Afterward, the DSSC sandwich was heated in an oven at 80°C for 5 minutes. This melted the thermoplastic sealant that binds the DSSC sandwich.

2.4 Characterizations

Fourier Transform Infrared (Shimadzu FTIR-8400) was used to identify chemical bonds by analyzing vibrational spectra of compounds at specific wavenumbers. In addition, FTIR was used for quantitative analysis to determine absorption peak intensities. The FTIR characterization involved analyzing the resulting spectrum for peaks corresponding to specific functional groups. The compound could absorb electromagnetic radiation in the infrared region, with wavenumbers ranging from 500 to 4000 cm^{-1}.

A UV-Vis spectrophotometer (UV-1600PC) was used to measure the dye's absorbance and that of the colored TiO_2. We characterized the dye sample photoanode by measuring absorbance from 200 to 800 nm. The characterization aimed to obtain absorbance values and wavelengths at which absorption occurred. These absorbance values were then used to calculate the Light Harvesting Efficiency (LHE) percentage and the sample band gap (Liu *et al.*, 2019). Meanwhile, to determine the morphology of the TiO_2 thin layer, the HitachiTM SU-3500 Scanning Electron Microscope (SEM) was used at PPNN ITB.

The data obtained were plotted into a graph depicting the wavelengths absorbed by this layer. Then, a plot of $\alpha h\nu^2$ against photon energy can be used to determine the band gap after determining the absorption coefficient (Mursyalaat *et al.*, 2023).

$$h\nu = 1240/\lambda \quad (1)$$

$$\alpha = A/l \quad (2)$$

$$\alpha h\nu^2 = K(h\nu - E_g) \quad (3)$$

λ is the wavelength, A is the absorbance, and l is the surface area. The band gap value can be determined by projecting a tangent to the curve, carried out with the x-axis intersection point $\alpha h\nu^2 = 0$ (Tauc, 1968; Tauc *et al.*, 1966). To find the percentage of LHE, we first determine the absorbance coefficient for each sample using Equation 2, then substitute it into Equation 4.

$$LHE\ (\%) = (1-10^{-\alpha}) \times 100\% \quad (4)$$

Cyclic voltammetry was used to determine the dye's LUMO and HOMO energy levels using a CS-310M electrochemical workstation (potentiostat/galvanostat). The test used three electrodes: glassy carbon as the working electrode, platinum as the counter electrode, and Ag/AgCl as the reference electrode. The electrolyte solution was 10 mL of 0.1 M KNO_3, which was dripped with dye; data were generated in the range -1.8 V to +1.8 V (Prima et al., 2024).

The data obtained from cyclic voltammetry, specifically the current and voltage values, were crucial for calculating the dye's band gap. We processed these values to determine the reduction and oxidation potential energies. We then used these values in Equations 5 and 6, underscoring the importance of cyclic voltammetry in our research. (Heinze, 1984; Nicholson, 1965).

$$HOMO = -(E_{ox} + 4.4) \quad (5)$$

$$LUMO = HOMO - E_g \quad (6)$$

The J-V characterization of the DSSC was conducted using the advanced Solar Standard Simulator AM 1.5G filter with ADCMT 6241A Source Meter, which provided precise measurements at 100 mW/cm^2 (Touihri et al., 2021). The results of this characterization were processed to obtain data on short-circuit current density (J_{sc}), open-circuit voltage (V_{oc}), fill factor (FF), and DSSC efficiency (η) using Equations 7 and 8 (Atia & Ahmed, 2023).

$$FF = (V_{max} \times J_{max})/(V_{oc} \times J_{sc}) \quad (7)$$

$$\eta = (V_{oc} \times J_{sc}) / P_{in} \times FF \quad (8)$$

The Jsc value was determined by measuring the current at zero voltage and dividing it by the layer's surface area. Similarly, the Voc value was determined by measuring the voltage at a near-zero current. The V_{max} and J_{max} values, representing the maximum power the DSSC can generate, were then determined. (Ghann et al., 2017; Pathak et al., 2019).

3. Results and Discussion

3.1 TiO_2 Microstructure Analysis

Scanning Electron Microscopy (SEM) was used to examine the surface morphology of the TiO_2 layer. As shown in Figure 1, the SEM image revealed that the TiO_2 surface was composed of mesoporous granules. ImageJ analysis confirmed the granule size, showing a particle size distribution with an average of 64 nm.

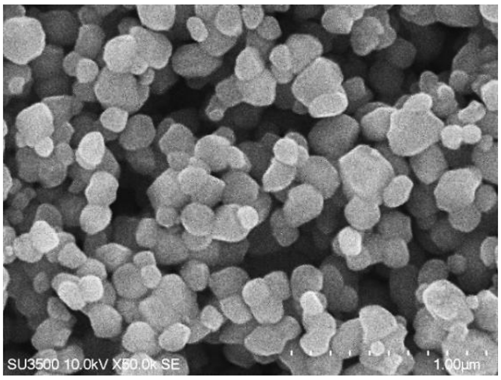

Fig 1. SEM image showing the surface morphology and particle distribution of the mesoporous TiO_2 thin film.

Specifically, the uniformity and small grain size help minimize aggregation, reducing dye adsorption on the TiO_2 surface. On the other hand, the crystalline structure of the TiO_2 nanoparticle surface can increase dye adsorption. In addition to pores, the thickness of the TiO_2 layer also affects dye absorption. In this study, the TiO_2 layer thickness was 9.1 μm, which is within the typical range for TiO_2 thin films, generally between 7 and 20 μm (Al-Bat'Hi *et al.*, 2018). Thicker TiO_2 layers generally increase dye adsorption. This is because a thicker layer provides a larger surface area for dye molecules to bind, thereby enhancing the overall dye-loading capacity. (Rahman *et al.*, 2020). Moreover, thicker TiO_2 layers can improve light absorption by increasing the light path length within the layer, increasing the probability of photon absorption by dye molecules. (Dissanayake *et al.*, 2020).

3.2 FTIR Analysis

The functional groups in Dewandaru fruit pigments must be identified to determine whether the fruit can be used as a colorant in DSSCs. Fourier transform infrared (FTIR) characterization produces transmittance spectra over the wavenumber range 4000 to 500 cm^{-1}, as shown in Figure 2. The graph was analyzed to determine the functional groups of dye constituent molecules.

There are 11 absorption peaks of this dye molecule, as shown in Figure 2. These peaks, summarized and analyzed in Table 1, are significant because they indicate specific functional groups in the molecule. In the single-bond region (2500-4000 cm^{-1}), there are 4 absorption peaks. The hydroxyl group (O-H) is indicated by peaks at wavenumbers 3433 cm^{-1}, 3418 cm^{-1}, and 3403 cm^{-1}. The peak at wavenumbers 2960- 2850 cm^{-1} indicates a C- H stretch of aliphatic groups, namely alkanes. Acetic acid as a solvent influences the presence of -COOH bonds from carboxyl groups at wavenumbers 2532 cm^{-1} and 2615 cm^{-1}. No absorption peaks were detected in the triple-bond region (2000-2500 cm^{-1}). In the double-bond region, two groups of peaks were detected: at 1721-1728 cm^{-1}, corresponding to carbonyl groups (C=O), and at 1634-1643 cm^{-1}, corresponding to stretching vibrations of aromatic double bonds (C=C).

Several peaks appear in the fingerprint region, between 500 and 1500 cm^{-1}. Peaks at wavenumbers 1404 cm^{-1} and 1396 cm^{-1} are due to C-H bonds from alkanes. (Golshan *et al.,* 2021; Shalini Singh et al., 2021). C-O bonds of ether groups were detected at 1000-1300 cm^{-1} wavenumbers (Unwakoly *et al.* 2025). At 677 cm^{-1} and 633 cm^{-1}, peaks indicate vibrations in aromatic C-H bonds (Nandiyanto *et al.*, 2019; Thummajitsakul & Silprasit, 2022).

The statistical analysis of FTIR absorption data for Dewandaru fruit pigments at pH levels (1.00, 1.66, 2.27, and

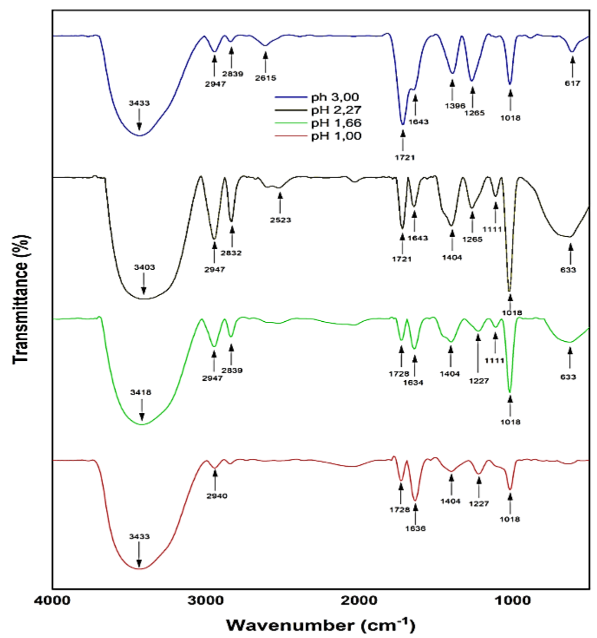

Fig 2. FTIR spectra of Dewandaru fruit extract solutions at various pH levels (1.00, 1.66, 2.27, and 3.00)

Table 1
Functional group identification and transmission percentages (T%) of Dewandaru fruit extract at various pH levels

pH 1.00		pH 1.66		pH 2.27		pH 3.00		Functional Group
$k\ (cm^{-1})$	T (%)	$k\ (cm^{-1})$	T (%)	$k\ (cm^{-1})$	T (%)	$k\ (cm^{-1})$	T (%)	
3433	15	3418	18	3403	6	3433	22	O-H hydroxyl
2940	94	2947	78	2947	52	2947	88	C-H alkane
-		2839	86	2832	66	2839	95	
-		-		2532	92	2615	92	-COOH carboxyl
1728	84	1728	83	1721	60	1721	31	C=O carbonyl
1636	69	1634	77	1643	77	1643	58	C=C aromatic
1404	91	1404	82	1404	62	1396	71	C-H alkane
1227	89	1227	90	1265	76	1265	65	
-		1111	93	1111	85	-		C-O ether
1018	77	1018	43	1018	11	1018	62	
-		633	82	633	54	617	88	C-H aromatic

3.00) reveals several trends in the transmission percentages (T%) of key functional groups. The C-H alkane group (2940 cm^{-1}) exhibits the highest transmission at pH 1.00 (94%). However, it decreases significantly at pH 2.27 (52%), indicating that this group's stability decreases as pH increases, though it recovers at pH 3.00 (88%). The carbonyl group (1728) exhibits its lowest transmission at pH 3.00 (31%), indicating that this functional group is most prominent and active at this pH. This suggests that pH 3.00 provides a more favorable environment for carbonyl-based binding compared to more acidic conditions (84% transmission at pH 1.00). The carboxyl group (2532 cm^{-1}) remains stable at pH 1.66 and pH 2.27 (both 92%), with no absorption at pH 1.00 and pH 3.00, highlighting its role in the mid-range pH environment. The O-H hydroxyl group (3433 cm^{-1}) shows variability, peaking at pH 3.00 (22%) but dipping at pH 2.27 (6%), suggesting that the hydroxyl group's contribution fluctuates with pH. Other groups, such as the ether (1227 cm^{-1}) and aromatic C-H (633 cm^{-1}), show a decreasing trend in transmission with increasing pH, with the ether group peaking at pH 1.66 (90%). The data indicate that functional groups such as C-H alkane and carbonyl groups are more stable in acidic environments. In contrast, the carboxyl group is most active at mid-range pH values, and the O-H hydroxyl group exhibits pH-dependent behavior. These trends suggest that pH plays a significant role in the stability and presence of these functional groups in Dewandaru pigments.

The functional groups in Table 1 correspond to the main functional groups that make up anthocyanin pigments. Mattioli *et al.* (2020) mentioned that at pH below 3, anthocyanins primarily exist in the form of red flavylium cations that carry a positive charge on oxygen. This can be due to hydroxyl and carbonyl groups that are stable under acidic conditions.

3.3 Effect of Dye Solution pH on Optical Characteristics of Active Materials

Figure 3a shows that the absorption rate, measured using a UV-VIS spectrophotometer with pH variation, is similar, but the intensities differ at some wavelengths. The absorption peak begins at 315-400 nm and increases until the optimal peak occurs at 400-480 nm, as shown in Table 2. The graph shows a decrease in absorption at 500 nm, indicating that the dye's absorption decreases from 500 to 700 nm. Therefore, the dye from dewandaru fruit extract can absorb ultraviolet and visible light, with optimal absorption at ultraviolet-A and purple and blue wavelengths.

The absorption intensity in the 300-500 nm wavelength range is highest for the dye solution at pH 3.00. This suggests that the dye solution's pH can influence the dye's absorption characteristics. While the difference in absorption intensity is negligible at other wavelengths, the dye solution's absorption decreases as acidity increases. This occurs because at low pH, dye molecules undergo protonation, which alters their electronic structure and reduces their ability to absorb light at specific wavelengths, thereby decreasing absorbance intensity. (Alkorta & Picazo, 2005). In addition, the dye has a conjugated system of closely spaced double bonds. Changes in pH can affect this system. For example, adding protons (H^+) at low pH can disrupt the conjugated double bond system, reducing color intensity. Protonation can significantly affect the conjugated π-electron system of dye molecules. This disruption can change the dyes' absorption spectra and color intensity (Mediantsev *et al.,* 2024). Anthocyanin pigment from mangosteen peel is reported to exhibit optimal absorption in the 400-480 nm range, with a peak around 430 nm (Pratiwi *et al.*, 2017).

The results of UV-VIS Spectroscopy testing on TiO_2 thin films that have been soaked in dye solution are shown in Figure

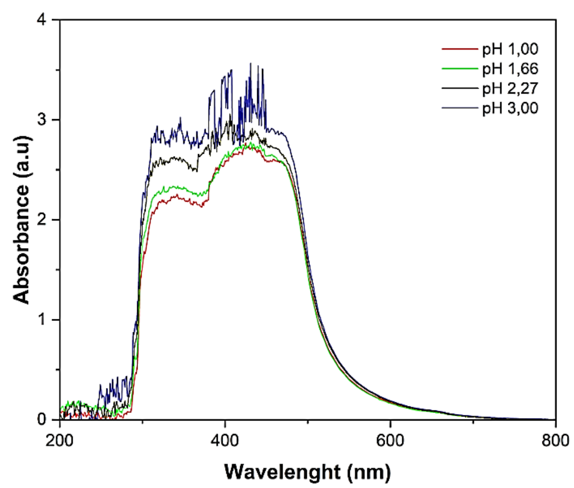

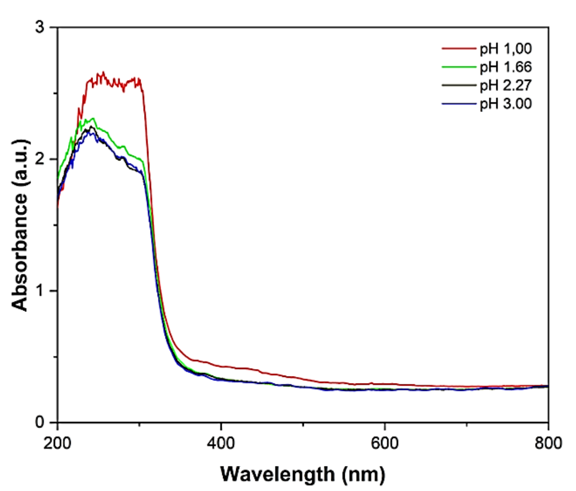

Fig 3. (a). UV-Vis absorption spectra of Dewandaru fruit extract solutions as a function of pH, (b) UV-Vis absorption spectra of films sensitized with Dewandaru extract at different pH levels

3b. The difference in absorption intensity is significant, as shown by TiO2 submerged in a dye solution at pH 1.00 in both the ultraviolet and visible regions. Absorption in ultraviolet light increased with the acidity of the dye solution applied to TiO_2 thin films. In the visible-light range, TiO2 submerged in dye solutions at pH 1.66, 2.27, and 3.00 showed similar absorption intensities. The absorption peak was detected at 250-350 nm, indicating a shift toward the visible range and a decrease in ultraviolet absorption intensity compared to the dye without TiO_2. This result shows that TiO_2 alters the dye's behavior, improving its light absorption in the UV and visible ranges. The peak shift and changes in absorption suggest that the interaction between TiO_2 and the dye is altering their optical properties. (Hegazy, 2019).

Yadav *et al.* (2021) reported that the intensity of visible light absorption increases after dye molecules are adsorbed on the TiO_2 surface. This indicates that interactions between dye molecules and TiO_2 can affect the dye's optical properties, increasing absorption intensity and shifting the absorption spectrum. Similarly, Pratiwi *et al.* (2016) report an increase in the absorption spectrum of TiO_2 thin films in the visible range, indicating that applying a dye to TiO_2. The surface can serve as a photosensitizer for DSSC absorption in this range. The absorption spectrum of TiO_2 as a function of pH provides valuable insights into the potential use of dye-TiO_2 systems in

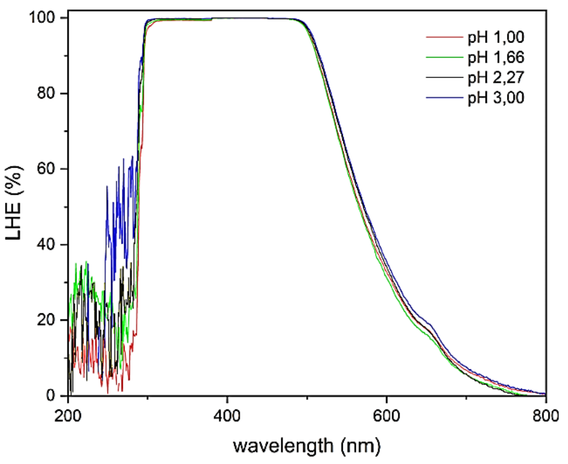

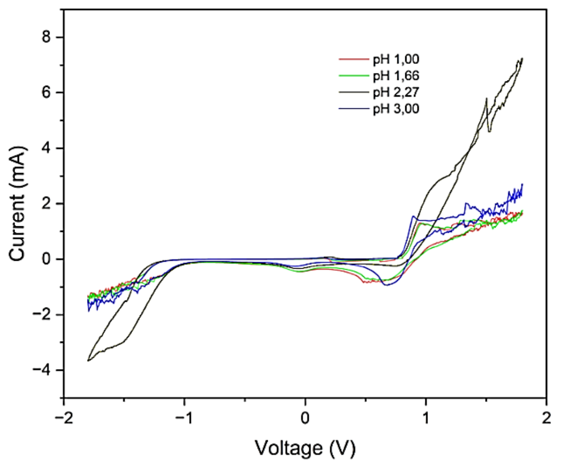

Fig 5. (a) Light harvesting efficiency (LHE) spectra of Dewandaru fruit extract at various pH levels, (b) Cyclic voltammograms of Dewandaru fruit extract at various pH levels to determine redox potentials

DSSCs. Table 2 summarizes the absorption peak data on the solution and TiO_2 samples.

We analyzed UV-Vis absorption data to determine the energy band values at each pH of the dye solution. Figure 4 shows the Tauc's Plot with the value of $(\alpha h\nu)^2$ on the y-axis and the energy value on the x-axis. Tauc's Plot analysis is performed by drawing a line that intersects the graph and the x-axis, yielding band gap values of 1.80 eV at pH 1.00, 1.81 eV at pH 1.66, 1.81 eV at pH 2.27, and 1.82 eV at pH 3.00.

The pH of the dye extractor solution affects the band gap. The band gap decreases as pH increases. (Saud et al., 2024). Increased acidity can cause dye molecules to break down. This occurs because dye molecules interact with hydrogen ions (H^+) in an acidic environment. As a result, the dye molecules break down into simpler compounds (Lozano-Alvarez *et al*., 2015).

Light absorption efficiency (LHE) is an optical property that influences DSSC performance. Figure 5a illustrates the light harvesting efficiency (LHE) at each wavelength, calculated using Equation 4. The data reveal that at pH 2.27, the LHE reaches its highest average of 34.85%, indicating optimal light-absorption efficiency under this acidic condition. In comparison, at pH 1.00, 1.66, and 3.00, the average LHE values are slightly lower, with 33.62%, 34.66%, and 33.55%, respectively. Although pH 1.66 is close to pH 2.27, efficiency at pH 1.00 and 3.00 is slightly lower, suggesting that pH 2.27 may offer the most favorable environment for light absorption. The similar values

Table 2
Maximum absorption wavelength (λ_{max}) and peak absorbance (A_{max}) for dye solutions and sensitized TiO_2 films

pH	Dye sample		TiO_2 + Dye sample	
	λ_{max} (nm)	A_{max} (a.u.)	λ_{max} (nm)	A_{max} (a.u.)
1.0	425	2.77	256	2.66
1.6	431	2.78	244	2.31
2.2	406	3.06	241	2.25
3.0	431	3.57	238	2.21

Table 3
Energy levels (HOMO/LUMO), optical band gaps, and average light harvesting efficiency (LHE) of Dewandaru dye at various pH levels

pH	HOMO (eV)	LUMO (eV)	Band gap (eV)	LHE (%)
1.0	-5.19	-3.39	1.80	33.62
1.6	-5.25	-3.44	1.81	34.66
2.2	-5.21	-3.40	1.81	34.85
3.0	-5.26	-3.44	1.82	33.55

observed at pH 1.00, 1.66, and 3.00 indicate that, while pH affects the LHE, the differences are not drastic, with pH 2.27 standing out as the condition with the highest efficiency. Figure 5b shows the results of the cyclic voltammetry Characterization test conducted to determine the voltage at which oxidation occurs in the dye molecule. By using Equation 5, the voltage is analyzed to determine the Highest Occupied Molecular Orbital (HOMO) level. At the same time, the Lowest Unoccupied Molecular Orbital (LUMO) level value is obtained by summing the HOMO value with the energy band gap value. The HOMO and LUMO values are summarized in Table 3.

The HOMO and LUMO values are not directly affected by acidity. pH variations affect the energy band gap width, thereby altering the HOMO and LUMO values of the dye sample. (Mikheev *et al*., 2017). Research conducted by Barbinta-Patrascu et al. (2024) reported similar results for the HOMO and LUMO values of Curcuma Longa extract, with HOMO and LUMO at pH 4.00 of -5.87 eV and -4.24 eV, and at pH 3.5 of -5.83 eV and -4.28 eV. At pH 3.0, the values were -5.91 eV and -4.22 eV, respectively.

3.4 Effect of Dye Solution pH on Performance of DSSC

J-V characterization testing under sunlight intensity was conducted to measure DSSC performance. The values of open-circuit voltage (Voc) and short-circuit current density (J_{sc}) were obtained from this test. Equation 8 is used to calculate the two values needed to determine the efficiency of each dye sample. This test was also carried out on a conventional dye sample, N719, for comparison.

DSSC samples with dye from Eugenia uniflora fruit with varying acidity levels produced Voc values between 0.32 and 0.42 Volts and Jsc values between 52 $\mu A/cm^2$ and 59 $\mu A/cm^2$. The highest Voc is observed in the DSSC sample at pH 3.00 (0.42 V). The most considerable Jsc value is observed in the DSSC sample at pH 1.66. Based on acidity, the Voc and Jsc values show no clear trend. This can occur when the HOMO and LUMO energy levels are well matched, thereby enabling efficient electron injection and dye regeneration (Conradie, 2024).

Table 4 shows that DSSC samples at pH 3.00 have the highest efficiency, which decreases as solution acidity increases.

Table 4
Photovoltaic parameters (V_{oc}, J_{sc}, FF, η) of *Eugenia uniflora*-sensitized DSSCs at different pH levels

pH	Voc (V)	Jsc (μA/cm²)	FF (%)	η (10^{-3} %)
1.00	0.360	52.5	48.4	9.15
1.66	0.319	58.6	63.9	11.93
2.27	0.379	54.4	66.1	13.42
3.00	0.425	53.0	68.7	15.48

Table 5
Comparative performance of Dewandaru-based DSSCs with synthetic N719 and other natural sensitizers from the literature

Dye	Voc (V)	Jsc (mA/cm²)	FF (%)	η (%)	Ref.
Eugenia uniflora, pH 1,00	0.360	0.0525	48.4	0.00915	-
Eugenia uniflora, pH 1,66	0.319	0.0586	63.9	0.01193	-
Eugenia uniflora, pH 2,27	0.379	0.0544	66.1	0.01342	-
Eugenia uniflora, pH 3,00	0.425	0.0530	68.7	0.01548	-
N719	0.694	8.23	61.1	3.49212	-
N719	0.846	17.73	75.0	11.18	(Conradie, 2024)
Oryza sativa + N719	0.558	5.69	61.3	1.95	(Prima et al., 2020)
Brassica oleracea, pH 2,00	0.533	1.449	71.1	0.555	(Chien & Hsu, 2013)
C.xanthorrhiza + A. cordiofoli, pH 1,77	0.320	2.5	-	0.096	(Setiarso et al., 2023)

In addition to the direct influence of Voc and Jsc, the efficiency is also indirectly affected by the fill factor. (Conradie, 2024). Efficiency increases with increasing fill factor for each DSSC sample using Eugenia uniflora fruit extract dye. Research by Chien and Hsu (2013) found that the efficiency of anthocyanin dye from Brassica oleracea peaked at pH 8.00, and efficiency decreased as solvent acidity increased. Table 5 summarizes other research data for comparison.

For comparison, the DSSC using the conventional synthetic dye N719 achieved an efficiency of 3.49%, significantly higher than the best performance of the Dewandaru fruit extract dye (0.01548% at pH 3.00). As shown in Figure 6 and Table 5, there is a large gap in the short-circuit current density, with values of approximately 0.105 mA/cm² for Dewandaru and 8.23 mA/cm² for N719. The natural dye (Eugenia uniflora) shows lower light absorption and energy-conversion efficiency than the synthetic N719 dye, which has higher short-circuit current density (J_{sc}) and open-circuit voltage (Voc). N719 also shows improved charge-transfer and collection properties, enabling efficient electron injection into the TiO_2 semiconductor. While natural dyes offer environmental benefits, their efficiency lags behind that of synthetic dyes. Ongoing research aims to bridge this gap through various optimization strategies, including co-sensitization, electrode modifications, and improved dye extraction methods.

This significant performance difference stems from fundamental differences in photophysical and electrochemical mechanisms, as reflected in the J–V curve characteristics. The massive gap (nearly two orders of magnitude) is the cumulative result of several factors: (a) limitations in the light absorption spectrum and intensity of the natural extract, (b) lower electron injection efficiency into the conduction band, (c) rapid charge recombination, and (d) suboptimal dye regeneration in the natural dye system. While natural dyes offer environmental benefits and lower costs, N719 serves as a high-performance control that confirms these primary challenges. Furthermore, N719 performance provides a benchmark for future optimization of Dewandaru-based cells through strategies such as anthocyanin purification, dye interface engineering, or co-sensitizers (Kharkwal and Dhawan 2024).

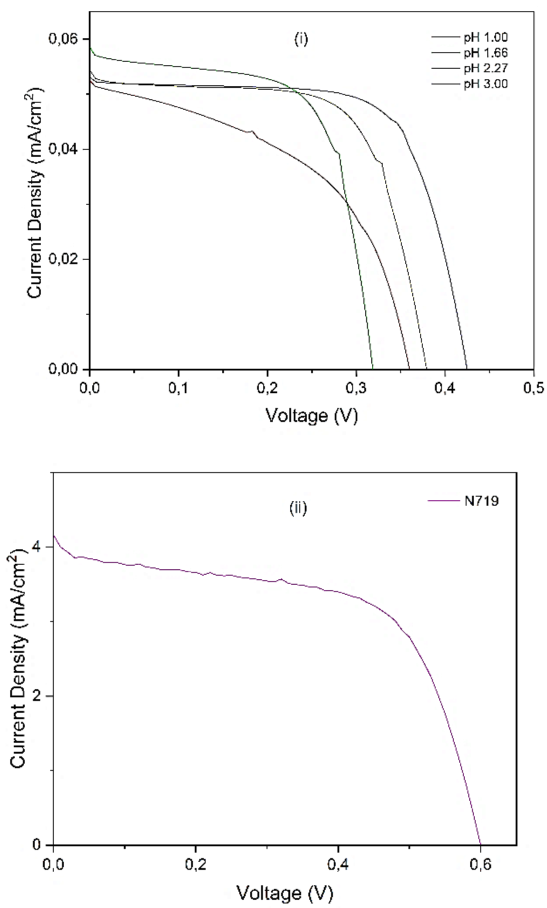

Fig 6. Photocurrent density-voltage (J-V) curves of DSSCs sensitized with: (i) Eugenia uniflora extract at various pH levels, and (ii) synthetic N719 dye

Table 6 presents the statistical analysis of pH effects on DSSC performance. The Pearson correlation was calculated

Table 6
Pearson correlation analysis of the effect of pH on the optical and photovoltaic performance of Dewandaru-based DSSCs

Pearson Correlation		pH	Dye absorbance	BandGap	LHE	Voc	Jsc	FF	HOMO	LUMO	η
η	Correlation Coefficient	0.993**	0.885	0.970*	0.063	0.668	-0.009	0.935	-0.733	-0.620	1**
	Sig. (2-tailed)	0.007	0.115	0.030	0.937	0.332	0.991	0.065	0.267	0.380	0.007
	N	4	4	4	4	4	4	4	4	4	4

**. Correlation is significant at the 0.01 level (2-tailed).
*. Correlation is significant at the 0.05 level (2-tailed).

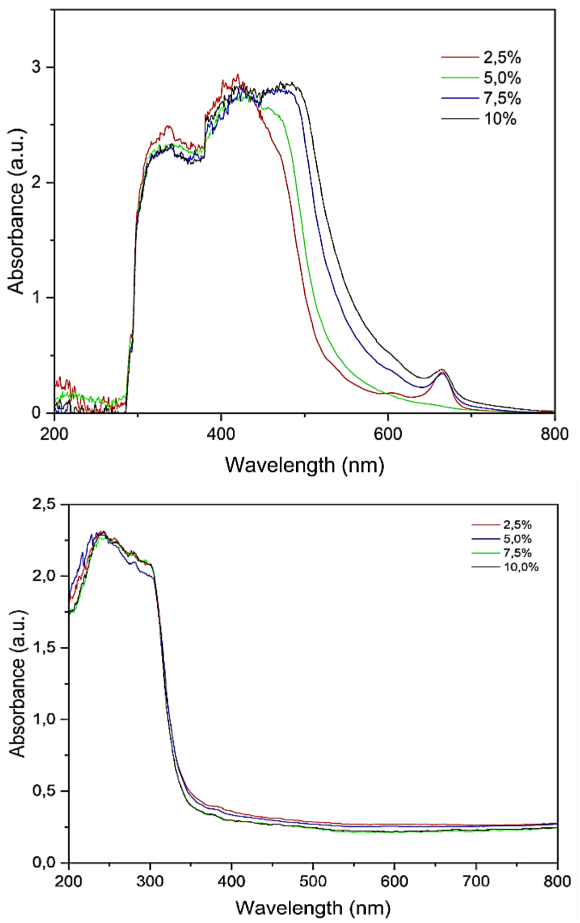

Fig 7. (a) UV-Vis absorption spectra of Dewandaru fruit extract at various concentrations (2.5% to 10%). (b) UV-Vis absorption spectra of TiO_2 films sensitized with Dewandaru extract at various concentrations

using a sample size of, representing the four pH variations tested. The analysis reveals highly significant correlations between pH and several key optical characteristics and performance parameters. The Pearson correlation coefficient for pH and the dye's efficiency (η) was 0.993, which is highly significant (p = 0.007), indicating a strong positive correlation between the pH of the dye solution and DSSC efficiency. This suggests that as pH increases, DSSC efficiency also improves, consistent with the performance trends observed in the study by Isah et al. (2015). The correlation between pH and dye absorbance was also substantial (r = 0.885). However, it was not statistically significant (p = 0.115), indicating that while there is a positive relationship between pH and dye absorbance, the effect is not significant.

This effect is less pronounced than that on efficiency. In contrast, pH and band gap energy showed a significant positive correlation (r = 0.970, p = 0.030), suggesting that changes in pH directly influence the dye's band gap energy and, in turn, DSSC performance.

Interestingly, the correlation between pH and light-harvesting efficiency (LHE) was weak and statistically insignificant (r = 0.063, p = 0.937), indicating that pH had little impact on this optical characteristic. Similarly, while pH showed a moderate positive correlation with Voc (0.668), Jsc (-0.009), and HOMO (0.935), these were not statistically significant (p = 0.332, p = 0.991, and p = 0.065, respectively). This suggests that while pH may influence these parameters, its effect is less strong and less consistent than on efficiency and band gap energy. Similarly, the band gap of theaflavin in the black tea waste extract (BTE) decreased by 0.17 eV when the pH was lowered. (Kumara et al., 2015).

The correlations between pH and LUMO (-0.733) and between pH and fill factor (FF) (-0.620) were negative but not statistically significant (p = 0.267 and p = 0.380, respectively). This indicates that pH changes did not significantly affect these parameters. The statistical analysis shows that pH has a substantial positive effect on DSSC efficiency and band gap energy. At the same time, its effects on other parameters such as LHE, HOMO, Jsc, and FF are less pronounced or not statistically significant. These findings underscore the importance of optimizing the dye solution pH to enhance overall DSSC performance.

3.5 Effect of Dye Solution Concentration on Optical Characteristics

Figure 7a shows the dye absorption as a function of wavelength in the visible and ultraviolet ranges. The dye samples in this variation exhibit nearly identical absorption intensities, particularly in the 380-450 nm region (Table 7). However, in the 450-650 nm wavelength range, the absorption area widens, and the absorption intensity increases with increasing dye concentration. Concentration variations in dragon fruit peel extract reported similar results: in the visible light range, the area widened, and absorption intensity increased. (Faqih *et al.*, 2019). Changes in the absorption spectrum as dye concentration increases can result from interactions among dye molecules, most likely leading to aggregation. This aggregation causes a bathochromic effect, also known as a red shift. This shift to a longer wavelength results from changes in the dye molecule's electronic structure. (Conradie, 2024). Figure 7b shows that the absorption capacity of TiO_2 varies with pH and solvent concentration. A similar curve is observed, especially in the UV wavelength range. The absorption peak was detected in the 250-350 nm range across all variations.

Table 7
Maximum absorption wavelength (λm_{ax}) and peak absorbance (A_{max}) for samples with varying dye concentrations

Concentration	Dye sample		TiO_2 + dye sample	
	***λmax* (nm)**	**Amax (a.u.)**	***λmax* (nm)**	**Amax (a.u.)**
2.5%	420	2.94	243	2.32
5.0%	431	2.77	244	2.31
7.5%	426	2.82	239	2.27
10.0%	425	2.87	240	2.30

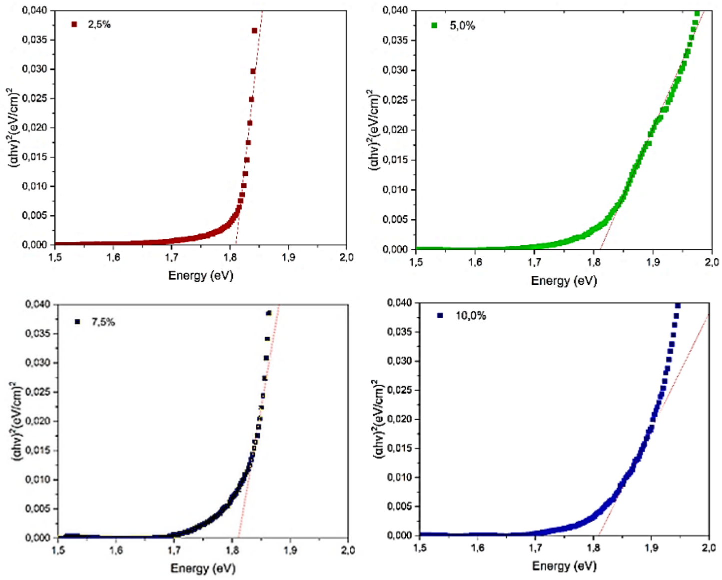

Fig 8. Tauc plots for optical band gap determination of Dewandaru dye at various concentrations

Table 7 summarizes the absorption peaks of the dye samples and TiO_2. Although the absorption curves look similar in the visible light range, absorption intensity differs slightly at concentrations of 2.5%, 5.0%, 10%, and 7.5%. Research on Binahong leaf extract with varying concentrations reported the results of absorption on TiO_2, with the order of absorption ability at a concentration of 5>3>1>10% (Muryani et al., 2019). According to Faqih et al. (2019)TiO_2's ability to bind dye molecules is limited, so increasing dye concentration does not consistently improve light absorption.

A Tauc plot is used to determine the band gap of the dye sample from its absorbance (Figure 8). Once the band gap is obtained, the HOMO and LUMO values can be determined. Tauc plot analysis showed that the optical band gap remained constant at 1.81 eV across all concentrations. This indicates that changes in dye concentration do not significantly shift the fundamental energy levels of the Dewandaru extract. Although higher concentrations typically lead to molecular aggregation, as shown by the broadening of the absorption spectrum and the bathochromic shift in Figure 7a, this aggregation appears to affect transition probabilities and absorption intensity rather than altering the intrinsic HOMO-LUMO gap. This observation is statistically supported by a Pearson correlation coefficient of 0.400 (p = 0.600), confirming that dye concentration has no significant impact on the band gap energy within the tested range of 2.5% to 10%.

Figure 9a shows the LHE graph of the dye at various concentrations. Data processing follows the pH variation: LHE values are averaged. The highest average LHE value, 40.19%, is achieved at a dye concentration of 10%. At the same time, the

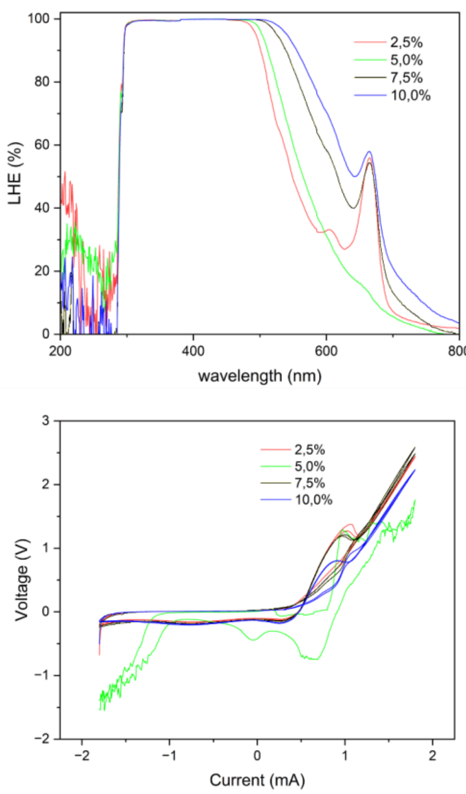

Fig 9. (a) Light harvesting efficiency (LHE) of Dewandaru dye samples as a function of extract concentration, (b) Cyclic voltammograms of Dewandaru fruit extract at different concentrations

Table 8
Energy levels and light harvesting efficiency (LHE) of Dewandaru dye at various extract concentrations

Concentration	HOMO (eV)	LUMO (eV)	Band gap (eV)	LHE (%)
2.5%	-5.07	-3.26	1.81	36.19
5.0%	-5.25	-3.44	1.81	34.66
7.5%	-5.12	-3.31	1.81	36.29
10%	-5.19	-3.38	1.81	40.19

concentration variations at 2.5%, 5.0%, and 7.5% have average values of 36.19%, 34.66%, and 36.29%, respectively. This indicates that while a higher dye concentration (10%) significantly increases LHE, lower concentrations yield relatively consistent but lower performance. These variations may reflect dye-interaction efficiency at different concentrations, with higher concentrations potentially saturating the medium and improving light absorption. In contrast, lower concentrations may be less effective at achieving similar results. Supported by Pradhan et al. (2023), Higher dye concentrations can lead to saturation, enhancing light absorption and overall efficiency. For instance, dye loading increases proportionally with concentration until saturation is reached, as observed at 0.2 mM D35.

Figure 13 shows the Cyclic voltammetry results at various concentrations. The HOMO level value at pH 1.00 is -5.07 eV; at pH 1.66 is -5.25 eV; at pH 2.27 is -5.12 eV; and at pH 3.00 is -5.19 eV. The LUMO value is obtained from processing the HOMO value using Equation (3.6). Table 8 summarizes the band gap, HOMO, LUMO, and average LHE values.

3.6 Effect of Dye Solution Concentration on DSSC Performance

DSSC performance was analyzed using pH variation experiments, and the same treatment was applied to analyze the effect of dye solution concentration on DSSC performance. Voc and Jsc values are used to determine the fill factor and DSSC efficiency.

The J-V curve shown in Figure 10 results from J-V characterization of DSSC devices with varying concentrations of dewandaru fruit extract dye solution. The Voc values for the four samples ranged from 0.32 to 0.46 V. Meanwhile, the Jsc values ranged from 66.2 to 105 μA/cm^2. Voc values with concentration variation show a trend: Voc7.5% > Voc10% > Voc2.5% > Voc5%. At the same time, Jsc values follow the trend Jsc10% > Jsc7.5% > Jsc2.5% > Jsc5%.

As the dye concentration increases, the light-absorbing area and intensity increase, which indirectly improves the value. The LHE value follows the same trend as the DSSC efficiency values, with the 10% sample achieving the highest efficiency of 0.0322%. Table 9 summarizes the detailed photovoltaic parameters at varying concentrations. While this concentration yielded the best performance in this study, its maximum efficiency of 0.0322% is significantly lower than that of other natural dyes, such as red cabbage (>1.4%). This performance gap is attributed to several chemical and physical limitations of

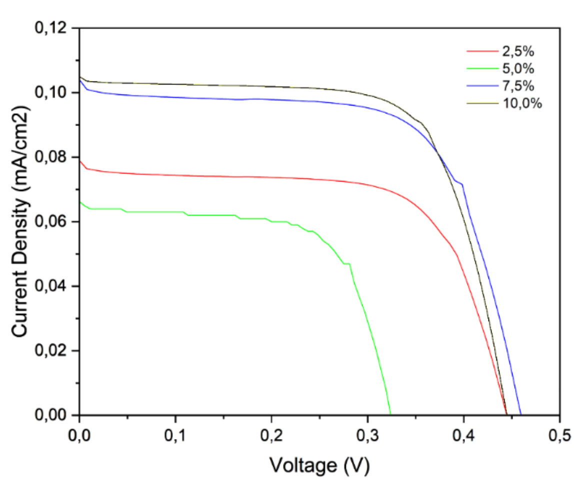

Fig 10. Photocurrent density-voltage (J-V) curves of DSSCs sensitized with Dewandaru extract at varying concentrations

the Dewandaru extract. First, the anthocyanins in Dewandaru show relatively weak binding and less homogeneous adsorption on the surface than more stable dyes.

Second, the low values indicate a high rate of charge recombination, in which injected electrons are likely to recombine with the electrolyte or with oxidized dye molecules due to the absence of strong anchoring groups, such as carboxyl or phosphonate groups. Third, Dewandaru's spectral response is primarily limited to the UV–blue region (400–480 nm), missing significant portions of the solar spectrum in the green–red range. Furthermore, using crude extract may introduce inactive compounds that act as charge traps.

These findings align with trends reported by Muryani *et al.* (2019) and Chien & Hsu (2013), where DSSC performance typically improves with dye concentration until an optimal point is reached. However, this peak efficiency is significantly lower than that of other natural sensitizers, such as red cabbage anthocyanins, which can exceed 1.4%. This performance gap is primarily attributed to several chemical and physical limitations inherent to the Dewandaru extract. First, although the anthocyanins in Dewandaru contain hydroxyl and carbonyl groups, their surface binding is dominated by relatively weak physical interactions and coordination bonds. Second, the low values suggest a high rate of charge recombination; the absence of strong anchoring groups, such as double –COOH or phosphonate, allows injected electrons to recombine more easily with the electrolyte or oxidized dye molecules. Third, Dewandaru's spectral response is primarily limited to the UV–blue region (±400–480 nm), failing to harvest the broader green–red region of the solar spectrum. Lastly, using a crude extract may introduce inactive compounds that act as charge traps or electron-transfer barriers. These findings highlight that while Dewandaru fruit extract is a viable natural sensitizer, its practical viability requires further optimization strategies, such as dye purification, surface treatment, or co-sensitization.

Table 9
Photovoltaic parameters of Eugenia uniflora-sensitized DSSCs at varying extract concentrations

Concentration	Voc (V)	Jsc (mA/cm^2)	FF (%)	Eff. (10^{-3} %)
2.5%	0.44	0.079	65.0	22.8
5.0%	0.32	0.066	63.9	11.9
7.5%	0.46	0.104	65.0	31.1
10.0%	0.45	0.105	69.0	32.2

Table 10.
Statistical analysis for the Concentration's Dye effect on DSSC performance

Pearson Correlation		Concentration	Dye absorbance	Band Gap	LHE	Voc	Jsc	FF	HOMO	LUMO	η
η	Corr. Coeff.	0.800	0.400	0.400	1.000*	0.800	1.000**	0.949	0.200	0.200	1.000
	Sig. (2-tailed)	0.200	0.600	0.600	0.000	0.200	0.000	0.051	0.800	0.800	0.000
	N	4	4	4	4	4	4	4	4	4	4

Table 10 presents the statistical analysis of the effect of concentration on DSSC performance. Using a sample size corresponding to the four concentration levels (2.5%, 5.0%, 7.5%, and 10.0%), the analysis reveals a perfect positive correlation between dye concentration and optical characteristics and performance parameters. The Pearson correlation coefficient for the concentration and dye efficiency (η) was 1.000, which is highly significant ($p = 0.000$), indicating a perfect positive correlation between the concentration of the dye solution and DSSC efficiency. This suggests that as the dye concentration increases, DSSC efficiency improves, highlighting the importance of concentration in optimizing DSSC performance.

The correlation between concentration and dye absorbance was moderate (r = 0.800). However, it was not statistically significant (p = 0.200), indicating that while concentration appears to influence dye absorbance, the effect was not strong enough to be statistically significant in this analysis. Similarly, the correlation between concentration and band gap energy (r = 0.400) was insignificant (p = 0.600), indicating that dye concentration did not significantly affect band gap energy.

In contrast, the correlation between concentration and light-harvesting efficiency (LHE) was highly significant ($r = 1.000$, $p = 0.000$), indicating a strong positive relationship. This suggests that higher dye concentrations significantly improve the DSSC's light-harvesting efficiency, which is crucial for maximizing the device's energy capture. The correlation between concentration and both Voc (0.800, $p = 0.200$) and J_{sc} (1.000, $p = 0.000$) was positive and significant, highlighting that concentration significantly affects these performance parameters, particularly Jsc, which showed a perfect correlation with concentration.

The correlation between concentration and fill factor (FF) was 0.949 ($p = 0.051$), indicating marginal statistical significance. This indicates that while concentration strongly influences the fill factor, the relationship is just shy of being definitively substantial at the 0.05 level. The correlations between concentration and HOMO and LUMO were both weak (0.200) and not statistically significant (p = 0.800), suggesting that concentration has little to no impact on these parameters in the context of DSSC performance.

In summary, the statistical analysis indicates that dye concentration significantly affects DSSC efficiency, light-harvesting efficiency, J_{sc}, and fill factor, with the most substantial impacts on efficiency and J_{sc}. However, concentration appears to have a smaller effect on dye absorbance, band gap energy, and HOMO/LUMO values. This suggests that optimizing the concentration of Dewandaru fruit extract in DSSC dye solutions is crucial for enhancing performance, particularly energy efficiency and light absorption.

Comparing these findings with those from Chien and Hsu (2013), which report that anthocyanin from red cabbage shows a high affinity for TiO_2 nanoparticles and achieves a light-to-electricity conversion efficiency of over 1.4%, significantly higher than the previously reported efficiencies of 0.5–0.6%, highlights the potential of natural dyes in DSSCs. In their study, optimizing factors such as pH, concentration, and immersion time was key to improving DSSC performance. Similarly, our study shows the importance of pH and concentration in optimizing DSSC performance. However, the maximum efficiency we observed (0.0322%) is lower than that reported by Chien & Hsu (2013), suggesting that further optimization, including exploring additional natural dyes or coadsorbents, could improve the performance of Dewandaru fruit extract-based DSSCs. Furthermore, the natural copigments in the crude extract, as observed by Chien & Hsu (2013), may enhance DSSC efficiency; future studies could explore this further.

3.7 Long-term Stability Considerations

A critical challenge for the practical application of natural dye-sensitized solar cells (DSSCs) is the long-term stability of the sensitizer, as natural pigments are notoriously susceptible to degradation. The anthocyanins in Dewandaru fruit extract are highly sensitive to external factors such as light, temperature, oxygen, and pH. Degradation typically involves transforming the colored flavylium cation into colorless carbinol bases or chalcones, reducing the cell's light-harvesting capability over time.

In this study, we intentionally used an acidic environment (pH 1.00–3.00), as anthocyanins are more stable in acidic conditions (pH < 7), where they predominantly exist as stable red flavylium cations. However, to enhance the practical lifespan of Dewandaru-based DSSCs beyond the laboratory scale, further stabilization strategies must be implemented. These include using UV-blocking filters to prevent photodegradation, co-pigmentation with more stable organic compounds to protect the anthocyanin structure, and advanced device encapsulation to minimize exposure to atmospheric oxygen and moisture. Addressing these stability issues remains a primary focus of future research to optimize Dewandaru fruit extract as a sustainable alternative to synthetic dyes.

4. Conclusion

In conclusion, the study on the effects of solution pH and the concentration of Dewandaru fruit extract, used as a natural dye, on the optical characteristics and performance of DSSC demonstrated that both factors significantly influence device performance. pH variation affects absorption peak intensity, band gap energy, and HOMO and LUMO values, with optimal performance at pH 3.00, yielding a Voc of 0.425 V, Jsc of 0.053 mA/cm², a fill factor of 68.7%, and an efficiency of 0.01548%. As the solution's acidity increased, DSSC's performance decreased. The extract concentration did not notably affect the band gap energy, nor did it significantly impact the HOMO and LUMO values, as confirmed by the statistical analysis ($p = 0.800$). However, higher concentrations broadened the absorption region and slightly increased the LHE percentage. The best DSSC performance was achieved at a 10% concentration, yielding a Voc of 0.45 V, Jsc of 0.105 mA/cm², a fill factor of 69.0%, and an efficiency of 0.0322%. This study shows that both solution pH and extract concentration play crucial roles in optimizing optical properties and enhancing DSSC performance. Further optimization of the solution pH and extract concentration should be explored to improve the efficiency of Dewandaru fruit extract-based DSSCs. Additional factors, such as immersion time and coadsorbents, could enhance performance. Future research could also examine the role of natural copigments in the crude extract, which may contribute to improved light-to-electricity conversion. Additionally, exploring different extraction methods and using other natural dyes could improve the DSSC's optical properties and overall efficiency.

Acknowledgments

This research is funded by Universitas Pendidikan Indonesia through the research program of Research Grant for QS Ranking Improvement (RQS) with Contract No. 667/UN40.F7/PT.01.01/2026.

Author Contributions: Dadi Rusdiana: Conceptualization; Eka Cahya Prima: Methodology, Formal Analysis, Writing- Original Draft; Muhammad N Ikhsan: C-V analysis and DSSC performance analysis; Andhy Setiawan and Endi Suhendi: Project Administration, Validation; Aramel and Arip Nurahman: Semuel Unwakoly: Layout and editing. All authors have read and agreed to the published version of the manuscript.

Conflicts of Interest: The authors declare no conflict of interest.

References

Al-Bat'Hi, S. A. M., Ahmed, N., Othman, R., & Othman, M. (2018). Optimization of TiO2 thin film thickness for dye sensitized solar cell applications. *IOP Conference Series: Materials Science and Engineering*, https://doi.org/10.1088/1757-899X/290/1/012004

Alessa, A. H., Alqarni, S. A., Qurban, J., Alghasham, H. A., Ashour, G. R. S., Bayazeed, A., Alharbi, A., & El-Metwaly, N. M. (2024). Synergistic Co-sensitization: Unlocking the potential of carbohydrazide chromophores and metal complexes for high-performance dye-sensitized solar cells [Article]. *Journal of Molecular Liquids, 408*, Article 125354. https://doi.org/10.1016/j.molliq.2024.125354

Alkorta, I., & Picazo, O. (2005). Influence of protonation on the properties derived from electron density. *Arkivoc, 9*, 305-320. https://doi.org/10.3998/ark.5550190.0006.926

Atia, D. M., & Ahmed, N. M. (2023). Mathematical modeling, parameter identification, and electrical performance of a DSSC based on nature-inspired optimization techniques [Article]. *Journal of Computational Electronics, 22*(2), 723-741. https://doi.org/10.1007/s10825-023-02018-8

Bagetti, M., Facco, E. M. P., Piccolo, J., Hirsch, G. E., Rodriguez-Amaya, D., Kobori, C. N., Vizzotto, M., & Emanuelli, T. (2011). Physicochemical characterization and antioxidant capacity of pitanga fruits (Eugenia uniflora L.). *Food Science and Technology, 31*, 147-154. https://doi.org/10.1590/S0101-20612011000100021

Barbinta-Patrascu, M.-E., Bita, B., & Negut, I. (2024). From nature to technology: Exploring the potential of plant-based materials and modified plants in biomimetics, bionics, and green innovations. *Biomimetics, 9*(7), 390. https://doi.org/10.3390/biomimetics9070390

Bekele, E. T., & Sintayehu, Y. D. (2022, 2022/10/14). Recent Progress, Advancements, and Efficiency Improvement Techniques of Natural Plant Pigment-Based Photosensitizers for Dye-Sensitized Solar Cells. *Journal of Nanomaterials, 2022*, 1024100. https://doi.org/10.1155/2022/1024100

Bhogaita, M., Shukla, A., & Nalini, R. P. (2016). Recent advances in hybrid solar cells based on natural dye extracts from Indian plant pigment as sensitizers. *Solar Energy, 137*, 212-224. https://doi.org/10.1016/j.solener.2016.08.003

Calogero, G., Bartolotta, A., Di Marco, G., Di Carlo, A., & Bonaccorso, F. (2015). Vegetable-based dye-sensitized solar cells [10.1039/C4CS00309H]. *Chem. Soc. Rev. , 44*(10), 3244-3294. https://doi.org/10.1039/C4CS00309H

Carella, A., Borbone, F., & Centore, R. (2018). Research progress on photosensitizers for DSSC. *Frontiers in chemistry, 6*, 481. https://doi.org/10.3389/fchem.2018.00481

Chen, D., Fan, G., Zhu, W., Yang, H., Xi, H., He, F., Lin, Z., Zhang, J., Zhang, C., & Hao, Y. (2020). Highly efficient bifacial CsPbIBr 2 solar cells with a TeO 2/Ag transparent electrode and unsymmetrical carrier transport behavior. *Dalton Transactions, 49*(18), 6012-6019. https://doi.org/10.1039/D0DT00407C

Chen, D., He, Y., Fan, G., Zhang, Z., Zhu, W., Xi, H., Zhou, L., Zhang, C., Zhang, J., & Hao, Y. (2023). Ultrahigh fill-factor all-inorganic CsPbBr3 perovskite solar cells processed from two-step solution method and solvent additive strategy. *Journal of Materiomics, 9*(4), 717-724. https://doi.org/10.1016/j.jmat.2023.01.012

Chien, C.-Y., & Hsu, B.-D. (2013, 12//). Optimization of the dye-sensitized solar cell with anthocyanin as photosensitizer. *Solar Energy, 98, Part C*, 203-211. https://doi.org/10.1016/j.solener.2013.09.035

Conradie, J. (2024). Effective dyes for DSSCs–Important experimental and calculated parameters. *Energy Nexus*, 100282. https://doi.org/10.1016/j.nexus.2024.100282

da Silva Diniz, P. R., Rispoli, R. G., Minozzo, M. M., Jobim, L. H., Junges, M., & Stefenon, V. M. (2014). A regenerative route for Eugenia unifloraL. (Myrtaceae) through in vitro germination and micropropagation [Article]. *Annals of Forest Research, 57*(1), 39-45. https://doi.org/10.15287/afr.2014.179

Dissanayake, M. A. K. L., Senthuran, S., & Senadeera, G. K. R. (2020). Efficiency enhancement in dye-sensitized solar cells using hierarchical TiO2 submicron size spheres as a light scattering layer [Article]. *Journal of Solid State Electrochemistry, 24*(10), 2261-2269. https://doi.org/10.1007/s10008-020-04727-7

Eka, C. P., Yuliarto, B., & Suyatman, S. (2013). Performance of Natural Carotenoids from Musa aromatica and Citrus medica var Lemon as Photosensitizers for Dye-Sensitized Solar Cells with TiO_2 Nanoparticle. *Adv. Mat. Res. , 789*, 167-170. https://doi.org/10.4028/www.scientific.net/AMR.789.167

Faqih, P., Aini, N., Mardhiyah, Z., & Nurosyid, F. (2019). Effect of concentration of red dragon fruit (Hylocereus costaricensis) peels extract as a dye of dye-sensitized solar cell (DSSC) on DSSC efficiency. AIP Conference Proceedings, https://doi.org/10.1063/1.5141733

Ghann, W., Kang, H., Sheikh, T., Yadav, S., Chavez-Gil, T., Nesbitt, F., & Uddin, J. (2017, 2017/01/27). Fabrication, Optimization and Characterization of Natural Dye Sensitized Solar Cell. *Scientific Reports, 7*(1), 41470. https://doi.org/10.1038/srep41470

Golshan, M., Osfouri, S., Azin, R., Jalali, T., & Moheimani, N. R. (2021). Co-sensitization of natural and low-cost dyes for efficient panchromatic light-harvesting using dye-sensitized solar cells. *Journal of Photochemistry and Photobiology A: Chemistry, 417*, 113345. https://doi.org/10.1016/j.jphotochem.2021.113345

Hegazy, A. (2019). High performance crystalline Tio2 mesocrystals for enhanced solar fuel. *Egyptian Journal of Chemistry, 62*(Special Issue (Part 1) Innovation in Chemistry), 115-122. https://doi.org/10.21608/ejchem.2019.13610.1841

Heinze, J. (1984). Cyclic Voltammetry—"Electrochemical Spectroscopy". New Analytical Methods (25). *Angewandte Chemie International Edition in English, 23*(11), 831-847. https://doi.org/10.1002/anie.198408313

Isah, K. U., Ahmadu, U., Idris, A., Kimpa, M. I., Uno, U. E., Ndamitso, M. M., & Alu, N. (2015). Betalain pigments as natural photosensitizers for dye-sensitized solar cells: The effect of dye pH on the photoelectric parameters [Review]. *Materials for Renewable and Sustainable Energy, 4*(1), Article 39. https://doi.org/10.1007/s40243-014-0039-0

Kabeyi, M. J. B., & Olanrewaju, O. A. (2022). Sustainable Energy Transition for Renewable and Low Carbon Grid Electricity Generation and Supply [Review]. *Frontiers in Energy Research, 9*, Article 743114. https://doi.org/10.3389/fenrg.2021.743114

Kumara, N., Lim, A., Lim, C. M., Petra, M. I., & Ekanayake, P. (2017). Recent progress and utilization of natural pigments in dye sensitized solar cells: A review. *Renewable and Sustainable Energy Reviews, 78*, 301-317. https://doi.org/10.1016/j.rser.2017.04.075

Kumara, N. T. R. N., Petrović, M., Peiris, D. S. U., Marie, Y. A., Vijila, C., Petra, M. I., Chandrakanthi, R. L. N., Lim, C. M., Hobley, J., & Ekanayake, P. (2015). Efficiency enhancement of Ixora floral dye sensitized solar cell by diminishing the pigments interactions. *Sol. Energy 117*, 36-45. http://dx.doi.org/10.1016/j.solener.2015.04.019

Liu, H., Liu, L., Fu, Y., Liu, E., & Xue, B. (2019). Theoretical Design of D-π-A-A Sensitizers with Narrow Band Gap and Broad Spectral Response Based on Boron Dipyrromethene for Dye-Sensitized Solar

Cells [Article]. *Journal of Chemical Information and Modeling, 59*(5), 2248-2256. https://doi.org/10.1021/acs.jcim.9b00187
López, J., Vega-Gálvez, A., Rodríguez, A., Uribe, E., & Díaz, P. (2017). Vacuum drying of Chilean murta (Ugni molinae Turcz) berries: Effect of temperature on kinetic parameters and assessment of energy consumption [Article]. *Journal of Food processing and Preservation, 41*(5), Article e13162. https://doi.org/10.1111/jfpp.13162
Lozano-Alvarez, J. A., Marañón-Ruiz, V. F., Jáuregui-Rincón, J., Medina-Ramírez, I., Frausto-Reyes, C., & Salinas-Gutiérrez, R. (2015). Removal of direct dyes with alginic acid [Article]. *Journal of the Mexican Chemical Society, 59*(3), 215-228. https://www.scopus.com/inward/record.uri?eid=2-s2.0-84957605164&partnerID=40&md5=32c506933143b85fb1b463d1da00e15d
Magalhães, C. G., Sola, I. M. M. S., Alberti, A., Ascari, J., & Nunes, D. S. (2025). Phenolic compounds and biological potential of Eugenia uniflora L.: A short review. *Eclética Química, 50.* https://doi.org/10.26850/1678-4618.eq.v50.2025.e1589
Maiaugree, W., Lowpa, S., Towannang, M., Rutphonsan, P., Tangtrakarn, A., Pimanpang, S., Maiaugree, P., Ratchapolthavisin, N., Sang-aroon, W., Jarernboon, W., & Amornkitbamrung, V. (2015, 10/13/online). A dye sensitized solar cell using natural counter electrode and natural dye derived from mangosteen peel waste [Article]. *Scientific Reports, 5*, 15230. https://doi.org/10.1038/srep15230
Mattioli, R., Francioso, A., Mosca, L., & Silva, P. (2020). Anthocyanins: A comprehensive review of their chemical properties and health effects on cardiovascular and neurodegenerative diseases. *Molecules, 25*(17), 3809. https://doi.org/10.3390/molecules25173809
Mediantsev, E., Dubinets, N., & Lobova, N. (2024). Computational Approach to the Study of Acidochromic Properties of Donor-π-Acceptor Systems Based on Dimethylamino-Substituted Dyes With Intramolecular Charge Transfer. *International Journal of Quantum Chemistry, 124*(19), e27488. https://doi.org/10.1002/qua.27488
Mikheev, Y. A., Guseva, L. N., & Ershov, Y. A. (2017). Transformations of methyl orange dimers in aqueous–acid solutions, according to UV–Vis spectroscopy data [Article]. *Russian Journal of Physical Chemistry A, 91*(10), 1896-1906. https://doi.org/10.1134/S0036024417090199
Mursyalaat, V., Variani, V. I., Arsyad, W. O. S., & Firihu, M. Z. (2023). The development of program for calculating the band gap energy of semiconductor material based on UV-Vis spectrum using delphi 7.0. Journal of Physics: Conference Series, https://doi.org/10.1088/1742-6596/2498/1/012042
Muryani, B., Sarifah, N., Kusumawardani, D., & Nurosyid, F. (2019). Effect concentration of dye solution binahong leaves to the efficiency of dye-sensitized solar cell (DSSC). AIP Conference Proceedings, https://doi.org/10.1063/1.5141735
Nandiyanto, A. B. D., Oktiani, R., & Ragadhita, R. (2019). How to read and interpret FTIR spectroscope of organic material. *Indonesian Journal of Science and Technology, 4*(1), 97-118. https://doi.org/10.17509/ijost.v4i1.15806
Nicholson, R. S. (1965, 1965/10/01). Theory and Application of Cyclic Voltammetry for Measurement of Electrode Reaction Kinetics. *Analytical Chemistry, 37*(11), 1351-1355. https://doi.org/10.1021/ac60230a016
O'Regan, B., & Grätzel, M. (1991). A low-cost, high-efficiency solar cell based on dye-sensitized colloidal TiO_2 films. *Nature, 353*, 737-740. https://doi.org/10.1038/353737a0
Omer, A. M. (2012). Sustainable Energy Development, the Role of Renewables and Global Warming. *J. Sust. Dev. Stud., 1*(1), 1-67.
Pathak, C., Surana, K., Shukla, V. K., & Singh, P. K. (2019). Fabrication and characterization of dye sensitized solar cell using natural dyes. *Materials Today: Proceedings, 12*, 665-670. https://doi.org/10.1016/j.matpr.2019.03.111
Pradhan, S. C., Velore, J., Meethal, S. M., & Soman, S. (2023). Fundamental Understanding of Dye Coverage and Performance in Dye-Sensitized Solar Cells Using Copper Electrolyte [Article]. *Energies, 16*(19), Article 6913. https://doi.org/10.3390/en16196913
Pramananda, V., Fityay, T. A. H., & Misran, E. (2021). Anthocyanin as natural dye in DSSC fabrication: A review. IOP Conference Series: Materials Science and Engineering, https://doi.org/10.1088/1757-899X/1122/1/012104
Pratiwi, D., Nurosyid, F., Supriyanto, A., & Suryana, R. (2017). Performance improvement of dye-sensitized solar cells (DSSC) by using dyes mixture from chlorophyll and anthocyanin. *Journal of Physics: Conference Series*, https://doi.org/10.1088/1742-6596/909/1/012025
Prima, E. C., Nugroho, H. S., Nugraha, Refantero, G., Panatarani, C., & Yuliarto, B. (2020). Performance of the dye-sensitized quasi-solid state solar cell with combined anthocyanin-ruthenium photosensitizer [10.1039/D0RA06550A]. *RSC Advances, 10*(60), 36873-36886. https://doi.org/10.1039/D0RA06550A
Prima, E. C., Nuruddin, A., Yuliarto, B., Kawamura, G., & Matsuda, A. (2018). Combined spectroscopic and TDDFT study of single-double anthocyanins for application in dye-sensitized solar cells. *New Journal of Chemistry, 42*(14), 11616-11628. https://doi.org/10.1039/C8NJ01202D
Prima, E. C., Rusliani, P. F., Suhendi, E., & Yuliarto, B. (2024). Performance of dye-sensitized solar cells with mixed three natural pigments and reduced graphene oxide as a counter electrode. *Results in Optics, 14*, 100592. https://doi.org/10.1016/j.rio.2023.100592
Rahman, M. F., Hidayat, A., & Diantoro, M. (2020). The influence of TiO2 film thickness in Dye-Sensitized Solar Cells (DSSC) performance based on TiO2/Ag@TiO2-ZnO. Journal of Physics: Conference Series, https://doi.org/10.1088/1742-6596/1572/1/012079
Rajkumar, S., Venkatraman, M., Arunkumar, A., & Jayaprakash, K. (2025). Anthocyanin and Betalain Pigments Assisted Green Synthesis of TiO_2: A Sustainable and Cost-Effective Approach for Dye-Sensitized Solar Cells Photoanodes. *Optical Materials*, 116710. https://doi.org/10.1016/j.optmat.2025.116710
Raturi, A., & Fepuleai, Y. (2010, 5//). Photosynthesis in a test tube- dye sensitized solar cells as a teaching tool. *Renewable Energy, 35*(5), 1010-1013. https://doi.org/10.1016/j.renene.2009.10.035
Santoso, P., Dewi, N. L. K. A. A., & Adrianta, A. (2020). Antioxidant capacity profile of dewandaru leaf (extract eugenia uniflora l.): part of usadha Bali. *International journal of life sciences, 4*(1), 87-98. https://doi.org/10.29332/ijls.v4n1.407
Saud, P. S., Bist, A., Kim, A. A., Yousef, A., Abutaleb, A., Park, M., Park, S.-J., & Pant, B. (2024). Dye-sensitized solar cells: Fundamentals, recent progress, and Optoelectrical properties improvement strategies. *Optical Materials, 150*, 115242. https://doi.org/10.1016/j.optmat.2024.115242
Seidemann, J. (2005). Surinam cherry (Eugenia uniflora L.) - A little known fruit [Article]. *Deutsche Lebensmittel-Rundschau, 101*(5), 204-209. https://www.scopus.com/inward/record.uri?eid=2-s2.0-20344393622&partnerID=40&md5=edb0f601c22b5648fa9d933d6ab670d1
Setiarso, P., Harsono, R. V., & Kusumawati, N. (2023). Fabrication of Dye Sensitized Solar Cell (DSSC) using combination of dyes extracted from Curcuma (Curcuma xanthorrhiza) rhizome and binahong (Anredera cordifolia) leaf with treatment in pH of the extraction. *Indonesian Journal of Chemistry, 23*(4), 924-936. https://doi.org/10.22146/ijc.77860
Sharma, D., Mehra, R., & Raj, B. (2022). Design and Analysis of Various Solar Cell Technologies for Improvements in Efficiencies [Article]. *Indian Journal of Engineering and Materials Sciences, 29*(5), 557-567. https://doi.org/10.56042/ijems.v29i5.51066
Singh, J., Gusain, A., Saxena, V., Chauhan, A. K., Veerender, P., Koiry, S. P., Jha, P., Jain, A., Aswal, D. K., & Gupta, S. K. (2013). XPS, UV–Vis, FTIR, and EXAFS Studies to Investigate the Binding Mechanism of N719 Dye onto Oxalic Acid Treated TiO2 and Its Implication on Photovoltaic Properties. *The Journal of Physical Chemistry C, 117*(41), 21096-21104. https://doi.org/10.1021/jp4062994
Singh, S., Maurya, I. C., Sharma, S., Kushwaha, S. P. S., Srivastava, P., & Bahadur, L. (2021). Application of new natural dyes extracted from Nasturtium flowers (Tropaeolum majus) as photosensitizer in dye-sensitized solar cells. *Optik, 243*, 167331. https://doi.org/10.1016/j.ijleo.2021.167331
Singh, S., Singh, P. K., Kakroo, S., Hachim, D. M., Dhapola, P. S., & Khan, Z. H. (2021). Eco-friendly dye sensitized solar cell using natural dye with solid polymer electrolyte as hole transport material. *Materials*

Today: Proceedings, 34, 760-766. https://doi.org/10.1016/j.matpr.2020.04.775

Sukarno, I., Matsumoto, H., Susanti, L., & Kimura, R. (2015). Urban energy consumption in a city of Indonesia: general overview. *International Journal of Energy Economics and Policy, 5*(1), 360.

Tauc, J. (1968). Optical properties and electronic structure of amorphous Ge and Si. *Materials Research Bulletin, 3*(1), 37-46. https://doi.org/10.1016/0025-5408(68)90023-8

Tauc, J., Grigorovici, R., & Vancu, A. (1966). Optical properties and electronic structure of amorphous germanium. *physica status solidi (b), 15*(2), 627-637. https://doi.org/10.1002/pssb.19660150224

Teja, A. S., Srivastava, A., Satrughna, J. A. K., Tiwari, M. K., Kanwade, A., Chand Yadav, S., & Shirage, P. M. (2023, 2023/02/01/). Optimal processing methodology for futuristic natural dye-sensitized solar cells and novel applications. *Dyes and Pigments, 210*, 110997. https://doi.org/10.1016/j.dyepig.2022.110997

Thummajitsakul, S., & Silprasit, K. (2022). Analysis of FTIR Spectra, Flavonoid Content and Anti-Tyrosinase Activity of Extracts and Lotion from Garcinia schomburgkiana by Multivariate Method. *Trends in Sciences, 19*(18), 5780-5780. https://doi.org/10.48048/tis.2022.5780

Touihri, A. E., Azizi, T., & Gharbi, R. (2021). Transient current effect on the dye sensitized solar cells I–V characterization [Article]. *IET Science, Measurement and Technology, 15*(1), 70-76. https://doi.org/10.1049/smt2.12007

Yadav, V., Negi, C. M. S., Kumar, D. K., & Gupta, S. K. (2021). Fabrication of eco-friendly, low-cost dye sensitized solar cells using harda fruit-based natural dye. *Optical Materials, 122*, 111800. https://doi.org/10.1016/j.optmat.2021.111800

Yan, Y., Zhang, Y., Zhao, Y., Ding, F., Lei, Y., Wang, Y., Zhou, J., & Kang, W. (2025). Review on TiO2 nanostructured photoanode and novel dyes for dye-sensitized solar cells application. *Journal of Materials Science*, 1-31. https://doi.org/10.1007/s10853-025-10734-8

Zhang, Z., Zhang, W., Wei, Z., Jiang, Q., Deng, M., Chai, W., Zhu, W., Zhang, C., You, H., & Zhang, J. (2020). Dipole-templated homogeneous grain growth of CsPbIBr2 films for efficient self-powered, all-inorganic photodetectors. *Solar Energy, 209*, 371-378. https://doi.org/10.1016/j.solener.2020.09.021